ISTITUTO NAZIONALE DI FISICA NUCLEARE

Sezione di Milano

INFN/TC–93/03
8 Aprile 1993

E. Acerbi, G.F. Ambrosio, L. Rossi:

CONSTRUCTION AND CALIBRATION OF AN APPARATUS FOR MAGNETORESISTANCE MEASUREMENTS OF FILAMENTS AND WIRES IN THE TEMPERATURE RANGE 1.7 – 300 K AND MAGNETIC FIELD UP TO 15 TESLA

PACS.: 07.20.Mc

Servizio Documentazione
dei Laboratori Nazionali di Frascati

INFN – Istituto Nazionale di Fisica Nucleare
Sezione di Milano

INFN/TC–93/03
8 Aprile 1993

CONSTRUCTION AND CALIBRATION OF AN APPARATUS FOR MAGNETORESISTANCE MEASUREMENTS OF FILAMENTS AND WIRES IN THE TEMPERATURE RANGE 1.7 - 300 K AND MAGNETIC FIELD UP TO 15 TESLA.

E.Acerbi, G.F.Ambrosio and L.Rossi

Dipartimento di Fisica dell'Universita' di Milano e INFN – Sezione di Milano, Laboratorio LASA, Via Fratelli Cervi 201, 20090 Segrate

ABSTRACT

An apparatus for measurements of electrical resistance under magnetic field up to 15 tesla has been built and operated. The temperature can vary between 1.7 K and 300 K. After calibration with copper wires, an investigation on $\rho = \rho(B,T)$ of NbTi thin filaments (especially intent for accelerator magnets) has started in order to investigate possible effects due to the small size and the capability of the Nb barrier to prevent sausaging.

Symbols

a-g, β	constants depending on Fermi surface and its orientation.
$\vec{B}$	magnetic induction vector (it usually lies along the z-axis).
$\vec{J}$	current density vector.
k	$=(\sigma_{zz}/\sigma_{xx})^{1/2}$.
l	electron mean free path in a bulk sample.
RRR	residual resistance ratio, we use: RRR=$\rho(293\,K)/\rho(4.2\,K)$.
T	absolute temperature.
γ	$=\omega_c\tau$: different sample of the same material behave in the same way as function of it.
$\rho(B,T)$	electrical resistivity.
ρ_0	electrical resistivity at B=0.
$\Delta\rho$	$=\rho(B)-\rho_0$: magnetoresistance.
$\sigma(B,T)$	electrical conductivity.
σ_0	electrical conductivity at B=0.
$\Delta(\sigma)$	conductivity tensor determinant.
τ	electron relaxation time.
ω_c	cyclotron frequency.

1 Introduction

For the new generation of particle accelerators, like LHC and SSC, the superconducting dipoles should generate magnetic fields ranging from 0.5 tesla to 10 tesla. At low fields, when beam is injected, the required field homogeneity is destroyed if the NbTi filaments have diameters larger than $7 \div 8\ \mu m$. Unfortunately when NbTi is drawn at so fine filaments its performance can be substantially reduced and even if a Nb barrier is put around the NbTi ingots (section of the Nb barrier can range between $2\% \div 5\%$ of the NbTi section) sausaging and other imperfections can be hardly avoided.

In the frame of the construction of the two first full size superconducting dipoles for the LHC [1,2] we have started a study to investigate different aspects of the superconductor needed for such a magnet.

In this paper we describe an apparatus able to measure the electrical resistance in magnetic field up to 15 tesla and in a wide temperature range from 1.7 K to 300 K. After calibration by means of almost pure copper wires, the apparatus is now used to investigate the behaviour of the NbTi wires, both without and with Nb barrier. The work, aimed to understand effects due to the small size of the NbTi filaments used for LHC, is under progress and the first measurements on superconductors produced by Vacuumschmelze (Hanau - D) and EM - LMI (Florence) are discussed.

This apparatus can also be used to measure magnetoresistance of small samples (preferable in thin wires) of Copper, Silver and all the other stabilizing materials used in superconducting wires and cables.

2 Theory

We recall that magnetoresistance is the change of electrical resistance in a sample, due to the application of a static, uniform, magnetic field. Resistivity can change in a great variety of ways, depending on such factors as the choice of the metal, whether the sample is monocrystalline or polycrystalline, the direction of magnetic field and current, the dimensions of the sample and, of course, the strength of the magnetic field. If current flows in the same direction of the magnetic field, we speak of longitudinal magnetoresistance while if current and field are perpendicular we speak of transverse magnetoresistance . In this case there is almost always a voltage (Hall voltage), in the third direction, the one perpendicular to both current and field. This is the Hall effect.

Usually magnetoresistance is positive (resistance increase together with the field), but it can be negative (size effects) or even oscillatory (size effects and quantum effects). When magnetoresistance is positive can show different behaviours vs. field: linear or quadratic, with or without saturation.

Of course magnetoresistance depends on samples temperature and purity. Temperature should be low enough to make thermal resistivity (due to scattering with phonons) negligible with respect to residual resistivity (due to scattering with impurity and dishomogeneity). Purity can be evaluated measuring the residual resistance ratio (RRR) which is the ratio between resistance at 300 kelvin and resistance at a temperature low enough to make negligible the thermal resistivity (usually 4.2 Kelvin). So the bigger RRR the better the sample. Actually the RRR is sensitive both to impurities and to lattice defects such as dislocation. By annealing the sample the defects can be eliminated. Strictly speaking RRR is defined using resistance at 273.15 K ($0°C$) but we will stick to the easier form RRR = R(room temp.)/R(4.2 K). According to Mathieson's rule the resistivity is the sum of many components: $\rho = \rho_i + \rho_d + \rho_{th} + \rho_B + ...$ where ρ_i = impurities, ρ_d = lattice defects, ρ_{th} = thermal (phonons), ρ_B = magnetoresistance. The residual resistivity is then $\rho_0 = \rho_i + \rho_d$ and $\rho_B = \Delta\rho$.

From a theoretical point of view, the easiest sample to study are monocrystalline samples without size effects. Those samples can be considered having a perfect and uniform lattice, and semiclassical model is a good instrument to study transport coefficients and their dependence on lattice, lattice orientation, and Fermi surface. For a quantitative analysis of these relationships, LAK[1] theory can be used, otherwise a good understanding can re reached through qualitative arguments starting from the Effective Path theory and using Kohler's rule ($\Delta\rho/\rho_0 = F_1(\omega_c\tau)$)[2] and Onsager's relations ($\sigma_{ij}(\vec{B}) = \sigma_{ji}(-\vec{B})$).

Anyway in both cases it can be seen that magnetoresistance behaviour is strictly linked to the shapes of the electron orbit and to electron density in each kind of orbits. These

[1] Lifshitz, Azbel' and Kaganov have been the first in discussing the relationship between the varieties of orbit and the magnetoresistance [3].

[2] Kohler's rule is very important from both a theoretical and an experimental point of view. It says that magnetoresistance of different samples of the same material, but with different degrees of purity (and so different RRR), behaves in the same way if regarded as function of $\gamma = \omega_c\tau$ (ω_c is the cyclotron frequency, while τ is the relaxation time; $\omega_c = eB/m$, and in the free electron model: $\omega_c\tau = B\sigma_0/ne$). So for each component of resistivity tensor it is: $\frac{\Delta\rho}{\rho_0} = F_1(\omega_c\tau)$, in which F_1 is a function depending only on material and lattice orientation. Other ways to express the same rule are: $\frac{\Delta\rho}{\rho_0} = F_2(\frac{B}{\rho_0})$ and $\frac{\Delta\rho}{\rho_0} = F_3(\frac{RRR\,B}{T})$. Kohler's rule breaks down when phonon scattering dominates, and when the effects of orbit quantization are observable.

orbits can be obtained sectioning the Fermi surface, in the repeated zone scheme[3], with plains normal to magnetic field direction. The possible orbits are: electron closed orbits (electrons turn around magnetic field as free electrons), hole closed orbits (electrons, passing through Fermi surface in different cells, turn as free positive particles), open orbits (may be periodic or not), and extended orbits (closed but very long).

It is demonstrated that *if all orbits are closed*, the high-field behaviour ($\gamma = \omega_c \tau \gg 1$)[2] of the conducting tensor, keeping only the leading terms, is:

$$\frac{\sigma_{ij}}{\sigma_0} \approx \begin{bmatrix} \frac{a}{\gamma^2} & \frac{d}{\gamma} & \frac{e}{\gamma} \\ -\frac{d}{\gamma} & \frac{b}{\gamma^2} & \frac{f}{\gamma} \\ -\frac{e}{\gamma} & -\frac{f}{\gamma} & c \end{bmatrix} \tag{1}$$

in which $a...f$ are constants depending on Fermi surface and its orientation, $\vec{B}$ is supposed parallel to z-axis, and $\gamma = \omega_c \tau$ is proportional to B. Inverting this tensor[4] it can be seen that:

$$\frac{\rho_{xx}}{\rho_0} \approx \frac{b}{d^2}\left(1 + \frac{f^2}{bc}\right) \quad \text{if d} \neq 0 \tag{2}$$

$$\frac{\rho_{xx}}{\rho_0} \div \gamma^2 \quad \text{se d} = 0 \tag{3}$$

Provided the Hall effect does not vanish (non compensated materials), d $\neq 0$ and transverse magnetoresistance (ρ_{xx} or ρ_{yy}) saturates at high field. This is the most common case. In compensated materials it is d $= 0$ and transverse magnetoresistance increases as γ^2 i.e. as B^2. This rise stops only when a magnetic breakdown changes electron density in some orbits. In case of extended orbits — which are closed, too — the behaviour is basically the same. However, since extended orbits are made up of many elementary units, cyclotron frequency (ω_c) is low and a correspondingly large field will be needed to reach saturation. Until this happens the resistivity continues to rise, so that $\Delta\rho_{xx}/\rho_0$ may reach large values.

In the case of open orbits the behaviour is different and we give the general form of the conductivity tensor in the high-field approximation, keeping only the leading terms. We suppose $\vec{B} \parallel z$-axis, as usual, and we choose as x-axis the line of open orbits in wave-vectors space so that in real space open orbits lie along y-axis[5] (usually there is only one set of open orbits at one time).

$$\frac{\sigma_{ij}}{\sigma_0} \approx \begin{bmatrix} \frac{a}{\gamma^2} & \frac{d}{\gamma} & \frac{e}{\gamma} \\ -\frac{d}{\gamma} & \beta & g \\ -\frac{e}{\gamma} & g & c \end{bmatrix} \tag{4}$$

from which:

$$\frac{\rho_{xx}}{\rho_0} \approx \frac{\beta c - g^2}{\Delta(\sigma)} \tag{5}$$

$$\frac{\rho_{yy}}{\rho_0} \approx \frac{ac + e^2}{\gamma^2 \Delta(\sigma)} \tag{6}$$

[3]It is the surface obtained putting in every reciprocal lattice cell a Fermi surface.

[4]ρ_{ij} is the inverse tensor of σ_{ij}. From a theoretical point of view it is easier to put boundary conditions on $\vec{E}$ and to see how $\vec{J}$ behaves. On the contrary, in real experiment boundary conditions are on $\vec{J}$. So theoretical studies give their results using σ_{ij}, while experiments give informations directly on ρ_{ij}.

[5]This happens because, under the action of a uniform magnetic field, the projections of the real-space orbits in a plane transverse to the field are the wave-vector-space orbits, rotated through 90° and scaled by the factor $\hbar/eB$.

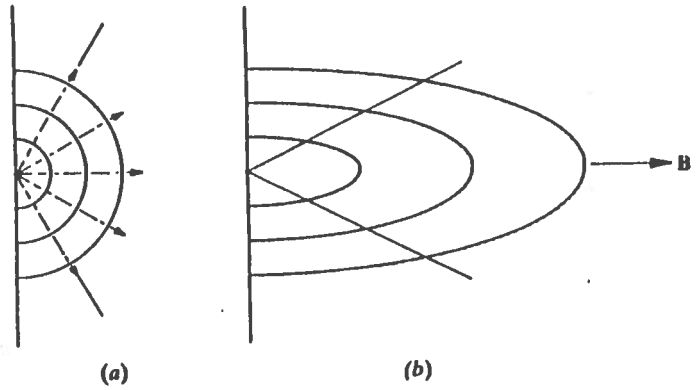

Figure 1: *Equipotential surfaces in an isotropic (a) and in a non isotropic material (b), from [4] pag. 43.*

Since the determinant $\Delta(\sigma)$ has a leading term proportional to $1/\gamma^2$, ρ_{xx} increases quadratically without limit, while ρ_{yy} saturates. It can be seen that it is only when $\vec{J}$ flows exactly along the open orbit direction in real space that this orbit can monopolize the current and allow the resistivity to saturate. If θ is the angle between the open orbit direction and the current flow direction (supposed x-axis), resistivity is:

$$\rho_{xx} \approx \frac{\gamma^2 \beta sin^2\theta}{a\beta + d^2} \tag{7}$$

showing the expected quadratic increase except when $\theta = 0$. On the contrary if there are two sets of open orbits normal to $\vec{B}$ and normal each other, transverse magnetoresistance always saturates.

At last, concerning *longitudinal magnetoresistance*, it should be said that its behaviour is strongly depending on the shape of Fermi surfaces and no general considerations can be outlined. Anyway field dependence is much weaker than for transverse magnetoresistance and usually there is saturation.

2.1 Current jetting

Before investigating the magnetoresistance behaviour in polycrystalls and in thine wires, it is important to point out same consequences of great anisotropy of conductivity. The most important consequence is current jetting, that is the strong preference for current to flow along $\vec{B}$ when $\sigma_{zz} \gg \sigma_{xx}$ ($z \parallel \vec{B}$). This effect can be very great, and must not be overlooked both in design of experiments to measure magnetoresistance and in theoretical considerations about magnetoresistance in polycrystals. In order to see this effect let's do the simplest example: a point contact injecting current into a semi-infinite sample whose plane surface is normal to $\vec{B}$, as in figure 1. Ignoring the Hall conductivity we have:

$$J_{\parallel} = \frac{B\sigma_1 z}{(r_\perp^2 + (z/k)^2)^{3/2}} \tag{8}$$

$$J_\perp = (\frac{r_\perp}{z}) J_{\parallel} \tag{9}$$

in which it is $k = (\sigma_{zz}/\sigma_{xx})^{\frac{1}{2}} \approx \omega_c \tau$, r is the distance from the injection point and $r_\perp$ its component transverse to the field. According to (9) $\vec{J}$ without the Hall current would diverge radially from the injection point, but (8) shows that it is not uniformly spread through the

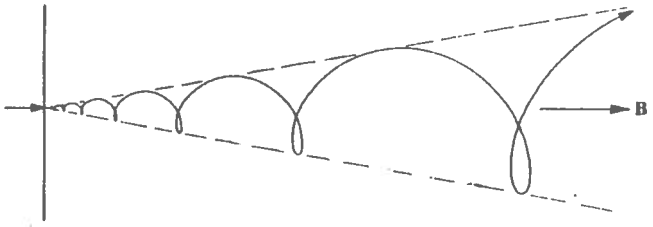

Figure 2: *A line of current flow for point injection when k=10, from [4] pag. 44.*

hemisphere. Integrating | J | leads to the result that the fraction of current lying within θ from the normal is

$$I_0 = 1 - \frac{1}{(1 + k^2 tan^2\theta)^{1/2}} \tag{10}$$

Half the current lies within a cone of semi-angle $\tilde{\theta} = tan^{-1}(\sqrt{3}/k)$ (e.g. for k=50,10,2 it is $\tilde{\theta}$=2,10,41 degrees). But this is not the complete description, for σ_{xy} (Hall conductivity) is likely to be considerably larger than σ_{xx} and will result in a strong circulating component of the current. The lines of current flow lie on cones as just described, but form helices, like that shown in figure 2.

2.2 Small angle scattering

At temperature low enough, resistivity is dominated by its residual components, but phonon scatterings are still present, and should be taken into account. Since phonons energy are very low at these temperatures, electrons absorbing or creating a phonon can be scattered through no more than a few degrees. So many scattering are necessary to destroy an organized current. A complete mathematical treatment of this problem is quite long[6], anyway it can be seen that small angle scattering effects become detectable at high magnetic fields, expecially increasing saturation values (the higher the temperature the higher these values).

2.3 Polycrystalline samples

The resistivity of a random polycrystalline mass, must be some sort of average over individual crystallites, but it is no easy matter to determine what average should be taken[7]. Of course if σ_{ij} or ρ_{ij} vary over a small range only, as orientation is changed with respect to $\vec{B}$ and $\vec{E}$, the choice of the averaging procedure will hardly matter, while if variations are great, result may change a lot. It can be seen[8] that because of current jetting, for longitudinal magnetoresistance with $\omega_c\tau$ values not too great it is necessary to average ρ, while for transverse magnetoresistance it is better to use σ; and experiments prove these considerations. But if $\omega_c\tau \gg 1$ (high magnetic fields) conductivity is dominated by open and extended orbits, (i.e.

[6]See for instance [4] pag. 125.

[7]If there is a lot of resistors (whose resistance is known) connected in series, the total resistance is the sum of all resistances. On the contrary, if they are connected in parallel the total conductivity is the sum of all conductivities; but if they are connected in a more complicated way, that we don' t know, it is impossible to calculate the total resistance (or conductivity). In order to make a prevision we have to understand which of the two behaviours prevails.

[8]See for instance [4] pages 178-181.

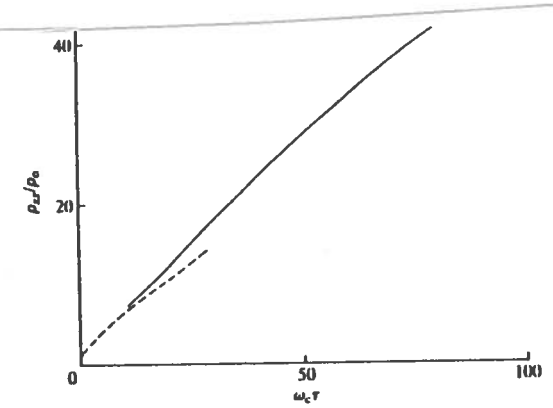

Figure 3: *Transverse magnetoresistance in a polycrystalline copper sample at 4 K from [7] (dotted line) and theoretical prediction in the high field limit from [6] (full line).*

see [5]), and every material, or better every kind of Fermi surface needs a particular study. In figure 3 it is shown the transverse magnetoresistance of a polycrystalline copper sample (dotted line) and the expected (see [6]) dependence to $\omega_c\tau$ ($\div B$), which is almost linear (full line). As shown in figure 3 the agreement with theoretical values is far from perfect. This is due to the fact that in polycrystalline copper, and in some other metals, Kohler' rule is not always obeyed. Deviations have been attributed to small-angle scattering, boundary scattering, magnetic impurities. In studying polycrystalline thin wires there is one more problem: in a drawn wire, even after annealing, there are preferred orientations, which can invalidate the assumption of randomness in crystallites distribution.

2.4 Size effects

In thin plates or in wires of small diameter, resistance is almost always enhanced by extra scattering of electrons by the surface, expecially if the mean free path in the bulk material is comparable to the transverse dimension of the sample. So in a wire with diameter (d) smaller than the bulk mean free path (l) the effective resistivity is expected to be[9]

$$\rho_{eff} = \rho_0 \frac{l}{d} \tag{11}$$

in which ρ_0 is the resistivity in the bulk material.

When diameter is almost equal to the bulk mean free path, the following formula can be used.

$$\rho_{eff} = \rho_0 l (\frac{1}{l} + \frac{1}{d}) \tag{12}$$

The quantity $\rho_0 l$ is an intrinsic property of the metal independent of l, being $\frac{\hbar k_F}{ne^2}$ for a free electron metal, $\frac{12\pi^3\hbar}{e^2 S}$ (in which S is Fermi surface area) for real metals.

The measured values of $\rho_0 l$ are quite variable (sensitive to temperature) and usually a little greater than the expected values. The reason is supposed to be small-angle scattering.

Size effects in presence of a magnetic field can give quite strange behaviours. If the field is parallel to the sample (a thin wire, we suppose) there are two different effects as B is increased: the magnetoresistance of the bulk material increases, while the contribution of boundary scattering decreases. This second effect is due to electron trajectories that become helices more and more narrow around the field, and so boundary scattering are reduced. In the limit of very high field the effective resistivity tends towards the bulk value, but at low fields the behaviour of longitudinal magnetoresistance depends on which effect dominates.

[9] See for instance [4] page 197.

In order to see a negative magnetoresistance sample must be very pure (i.e. $RRR > 1000$). Transverse magnetoresistance behaviour in thin plate (with thickness of the same order of the mean free path) is even more complicated. In fact also in this case there are two different effects that can be divided studying transverse magnetoresistance in thin plates. If the field is applied parallel to plate surface, magnetoresistance is like that seen before, while if the field is normal to the plate and the sample is very pure, some oscillations appear in the $(\rho - B)$ curve whose amplitude decays as B^{-2} (Sondheimer oscillations).
In a very pure thin wire both effect can appear.

3 Apparatus

The apparatus is made up by a superconducting magnet in which is inserted a variable temperature cryostat, where is put the sample holder. Temperature inside the insert is regulated using as refrigerant the liquid helium that is contained in the magnet, and as heater a proper resistance connected to an electronic temperature controller. Temperature is measured by two carbon glass sensors. The electrical resistance is measured by means of the standard four-terminals technique.

3.1 Magnet

The magnet providing the background field is a superconducting magnet able to generate field up to 13 tesla at 4.2 K and up to 15 tesla at 2.2 K. The field is generated by two superconducting coils in NbTi. Its intensity depends on the current that flows in the coils. This current is regulated with a precision of $\pm 0.3\ 10^{-5}$. The ratio between the field and the current is known within a relative error of $\pm\ 10^{-3}$. So magnetic field is known with a precision of 0.1 % and a stability greater than 0.01 %. Field homogeneity is very good, being 0.011 % on a sphere of radius 1 cm around the center.

Coils are contained into a cryostat that is insulated by a vacuum jacket, and a radiation shield cooled with liquid nitrogen. Usually coils are in a liquid helium bath at 4.2 K, but in order to reach fields in excess of 13 tesla, liquid helium is cooled down to 2.2 K by means of a λ-point refrigerator.

3.2 Variable temperature insert (VTI)

The gas flow variable temperature insert consists of two thin coaxial tubes made out of stainless steel. The outer is the vacuum chamber and the inner provides the useful space (Ø= 29 mm, h = 200 mm) where temperature is controlled (see figure 4). In the vacuum, between the two tubes, there is a copper radiation shield used in conjunction with optimised superinsulation to prevent a significant increase in radiative heat load on the helium bath when the VTI is operating at temperature substantially higher than the bath temperature. The temperature of the sample is determined by the temperature of the helium gas in which the sample is mounted. Liquid helium is sucked from the main reservoir through a needle valve (which is operated from the head of the cryostat), passes through a heat exchanger and enters into the sample space. For operation between 4.2 K and 300 K the liquid is evaporated in the heat exchanger by an heating element and the temperature of the outflowing gas is monitored by a carbon gas sensor (CGR). A temperature controller takes care of the temperature stabilisation. To work in this temperature range a constant

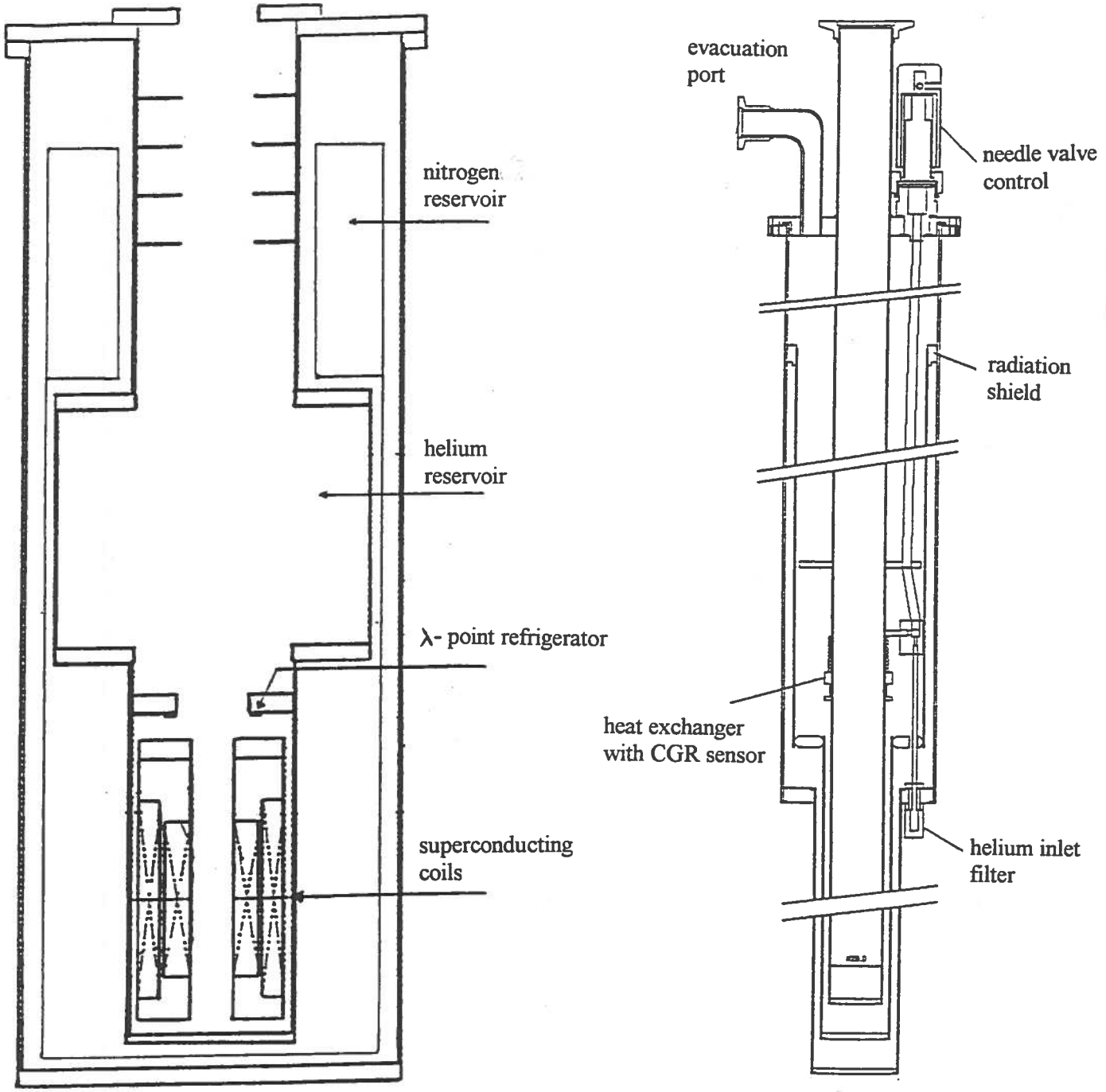

Figure 4: *Schematic section of the magnet and of the variable temperature insert (VTI).*

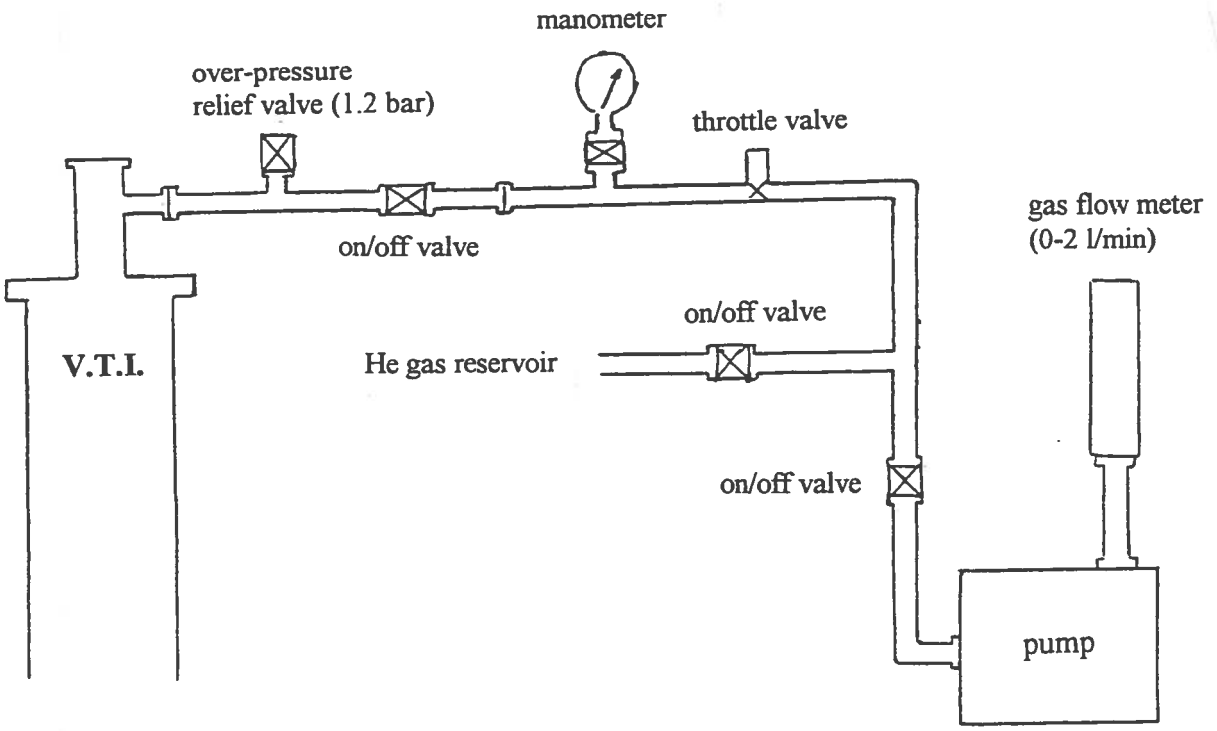

Figure 5: *Scheme of the pumping line on the VTI sample tube.*

gas flow between 0.1 and 0.3 litres/min through the VTI chamber is required, corresponding to a liquid consumption of approximately 10 cc/hour to 30 cc/hour. The gas flow rate is controlled by the use of a throttle valve on the pumping line (see figure 5), and of the needle valve. For rapid cooling this flow may be increased to 1 or 2 l/min, but this leads to a great temperature gradient in the sample tube which takes some time to stabilise. Once the gas flow has been set correctly, the temperature controller is used to regulate the action of the heater in order to reach and maintain the set temperature.

In order to operate at temperature below 4.2 K a different mode of operation is required. The volume below the heat exchanger should be allowed to fill with liquid helium by pumping on the sample space with the needle valve fully open. The valve should then be either closed or left very slightly open and the temperature of the sample changed by reducing the pressure over the small bath.

Sample temperature is always measured using a carbon glass sensor (CGR) put just above the sample holder.

3.3 Temperature control

The temperature controller we have used is a DRC-93CA model by Lakeshore which uses proportional, derivative and integral control circuitry (PID control technique) to determine the heating power. The heater is a 50 ohm resistance and can be fed with a current up to 1 A. So maximum power output is 50 W but to allow a fine control the max power can be reduced to 5 or 5 10^{-1} or 5 10^{-2} or 5 10^{-3} W. Parameters of PID control are set by user and can be changed every moment even during operation. Set point and sensors signals can be shown in their units (i.e. ohm for CGR sensors) or directly in kelvin.

The controller can store sensor calibration curves with up to 97 points for each curve. To control temperature it can use only one sensor at a time, but two sensor signals can be displayed together.

The sensors we use are two carbon glass resistors (CGR), one positioned near the heat

Table 1: *Field dependence of the CGR mounted on the sample holder at 4.30 K*

Field (T)	Temperature (K)	ΔT/T (%)
0	4.30	0
2	4.28	-0.5
4	4.26	-0.9
6	4.24	-1.4
8	4.22	-1.9
10	4.19	-2.6
12	4.15	-3.5

exchanger of the VTI, the other just above the sample holder. Both calibration curves have been set in controller's memory with more than 50 points for each one. Points have been chosen in such a way that the greatest temperature error is 0.011 K. Carbon glass sensors have been chosen since have the best precision and stability in this temperature range and in high magnetic field. However there is always a field dependence. We have measured it for the sensor near the sample at 4.2 K and results are shown in table 1. To keep temperature constant in the VTI during this control we let liquid helium fill the VTI sample space, and we made measurements, both increasing and decreasing the field many times, checking that temperature displayed by the sensor at B=0 didn't change.

In order to control temperature we have adopted this solution: as input sensor for the temperature controller we selected the one set near the VTI heat exchanger, while the other one was used to display the sample temperature. In this way thermal lag between the heat exchanger and the controlling sensor is very little, and a very good temperature control of the helium gas near them can be easily obtained. Once temperature in this region is constant, the system must be left stabilising till the temperature near the sample becomes equal to the set one. This procedure can need many minutes if a very good temperature stability is required. If the sensor near the sample is used as input for the temperature controller, the thermal path between the heater and the sensor becomes too long and thermal oscillations are hardly avoided.

The first solution has also another great advantage: the sensor on the VTI is far enough from the field not to feel field effects. So the first sensor is used to keep temperature constant, while the second sensor to monitor the temperature stability between measurements at the same field, and between groups of measurements by checking temperature values at B=0.

Working in this way, using maximum power output equal to 0.5 W (power -2) and Gain, Reset and Rate respectively equal to 4, 2 and 1, we have reached, a stability of ±0.02 K at different temperatures from 5 to 11 K (see table 5).

3.4 Sample holder and instrumentation

When a low resistivity sample is measured (like copper or NbTi in the transition region) the voltage drop along the sample is very low because the current must be kept low to avoid a significant heating of sample itself. In order to have a good signal well greater than noise, expecially for copper wires, the sample-holder has been designed for wires about ten cm long. Sample-holder is a little flat plate ($26 \times 10 \times 1\ mm^3$) made in fiberglass (G11) and with

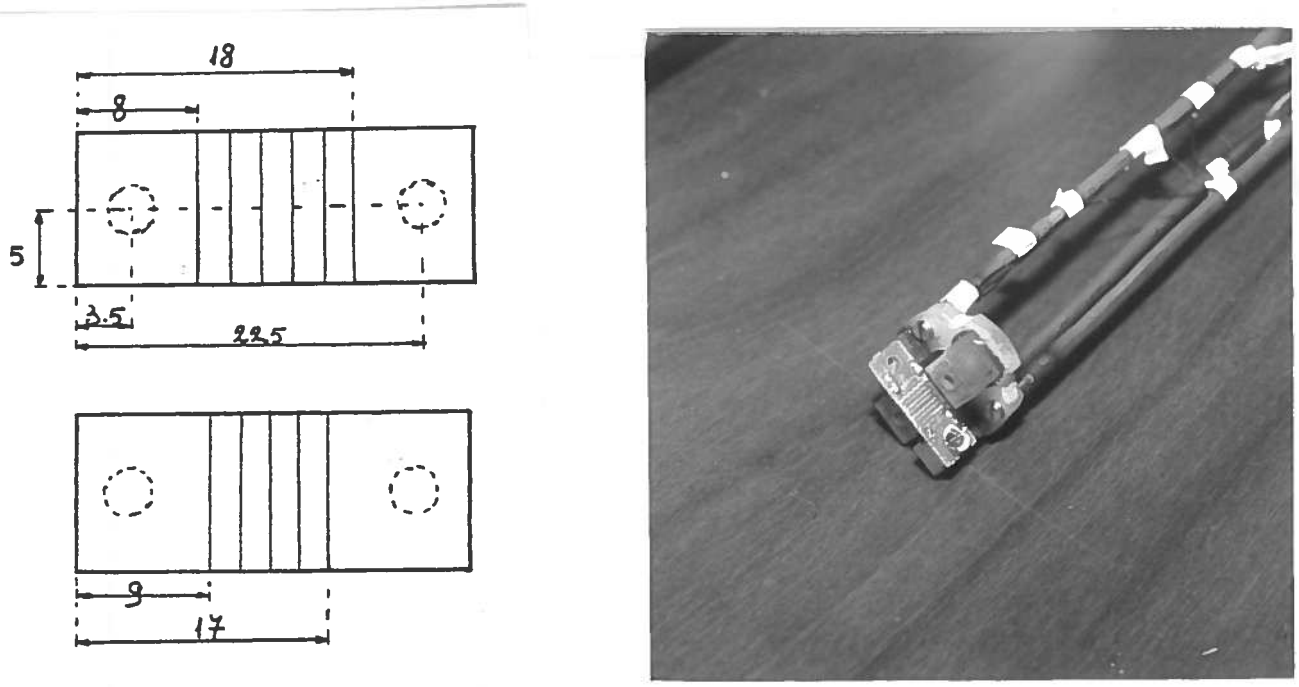

Figure 6: *A sketch of the sample-holder (dimensions in mm) with indication of the grooves for filaments, and a photograph of the bottom part of the support with the sample-holder set in longitudinal position.*

11 grooves, 0.3 mm deep, (6 on a face and 5 on the other) in which the wire is positioned around the holder. The sample-holder is kept in in the center of the magnetic field by a support and can be set both parallel and transverse to the magnetic field. The support is made by stainless steel 304 L (low carbon) tubes kept together by 5 fiberglass (G10) rings. Tubes are 4 mm in diameter and 0.2 mm thick, while rings external diameter is 28.5 mm. This support has been designed in order to let gas flow in VTI chamber, and to have a little heat conduction from the VTI top flange, where support is fixed, at room temperature, to the cold region near the sample. The wires used inside the VTI, both to bring current and to measure voltage, are $\vee = 0.2$ mm phosphor-bronze grade A alloy wires, insulated with a polyimide resin film. They have a low resistance (3.6 Ω/m at 300 K, 2.95 Ω/m at 77 K and 2.85 Ω/m at 4.2 K), a low thermal conductivity (71.13 W/m-K at 293 K), a very low magnetoresistance ($\delta R/R_0 \approx 6\ 10^{-5}$ at 4.2 K and 14 tesla) and can bring current up to 200 mA.

For the voltage measurements across the sample, a high sensitivity digital nanovoltmeter (Keithley 182 sdv) is used. Its best resolution is shown in table 2 as a function of signal intensity. The best resolution is obtained with the longest integration time (100 msec). This is the one we used, and in this configuration the precision of the nanovolmeter is 17 nV. This value has been verified making measures for 14 hours on a short-circuit.

To feed the sample different current generators have been used. With copper samples, fed with about 100 mA current, the power supply used had a current control and a stability of 0.04% and current intensity has been checked using a digital multimeter with a precision of 0.4% and a resolution of 10 μA. With the second NbTi wire, which need a current of about 0.1 mA, a power supply has been prepared able to generate current up to 2 mA with a stability better than 0.1%, while current intensity has been checked by means of a calibrated shunt (1 $K\Omega$); in this way resolution was 0.1 μA.

Table 2: *Maximum voltmeter resolution and measured precision.*

Range	Resolution	Precision
3 mV	1 nV	17 nV
30 mV	10 nV	
300 mV	100 nV	
3 V	1 μV	
30 V	10 μV	

4 Calibration and measurements

All measurements have been done with the sample-holder in both transversal and longitudinal position, in order to separate longitudinal and transverse magnetoresistance components. In fact, since the sample-holder used is not very thin (1 mm) respect to its height (10 mm), both components are present in every single measurement; but using two measures at the same temperature and field, with different sample-holder orientation, the components can be separated[10]. Here it is the system used:

$$\rho_{tra} = \frac{lV_{tra} - \frac{s}{2}V_{lon}}{l^2 + \frac{ls}{2} - \frac{s^2}{2}} \frac{1}{J} \tag{13}$$

$$\rho_{lon} = \left(\frac{V_{lon}}{J} - s\rho_{tra}\right)\frac{1}{l} \tag{14}$$

In which l and s are the total lengths of wire pieces on the longest and shortest face of sample-holder, V_{tra} and V_{lon} are the voltage measures at the same current when the field is perpendicular and parallel to the sample-holder. So if the sample-holder is set in longitudinal position l is the sum of all wire pieces that are parallel to the field and s of those that are transverse, while, if the sample-holder is perpendicular to the field, l is the sum of all transverse pieces and s of all the pieces that lie at 45^o with the field.

4.1 Copper samples

In order to cheek the apparatus we started measuring copper wires whose $\rho = \rho(T, B)$ is well established. We used two copper wires with diameters of 0.5 and 0.127 mm.

First sample (0.5 mm dia., 110 mm length) had a room-temperature resistance of 8.6 $m\Omega$ and so its resistivity was 1.54 10^{-8} Ωm. Its magnetoresistance has been investigated at 4.17 $\pm$ 0.05 K, using currents of 50, 100 and 150 mA in order to cheek possible self-heating effects, but no differences have been seen.

[10]This can be done in the hypothesis, commonly used, of no longitudinal-transverse coupling:

$$\rho = \begin{pmatrix} \rho_{tra} & \rho_{Hall} & 0 \\ -\rho_{Hall} & \rho_{tra} & 0 \\ 0 & 0 & \rho_{lon} \end{pmatrix}$$

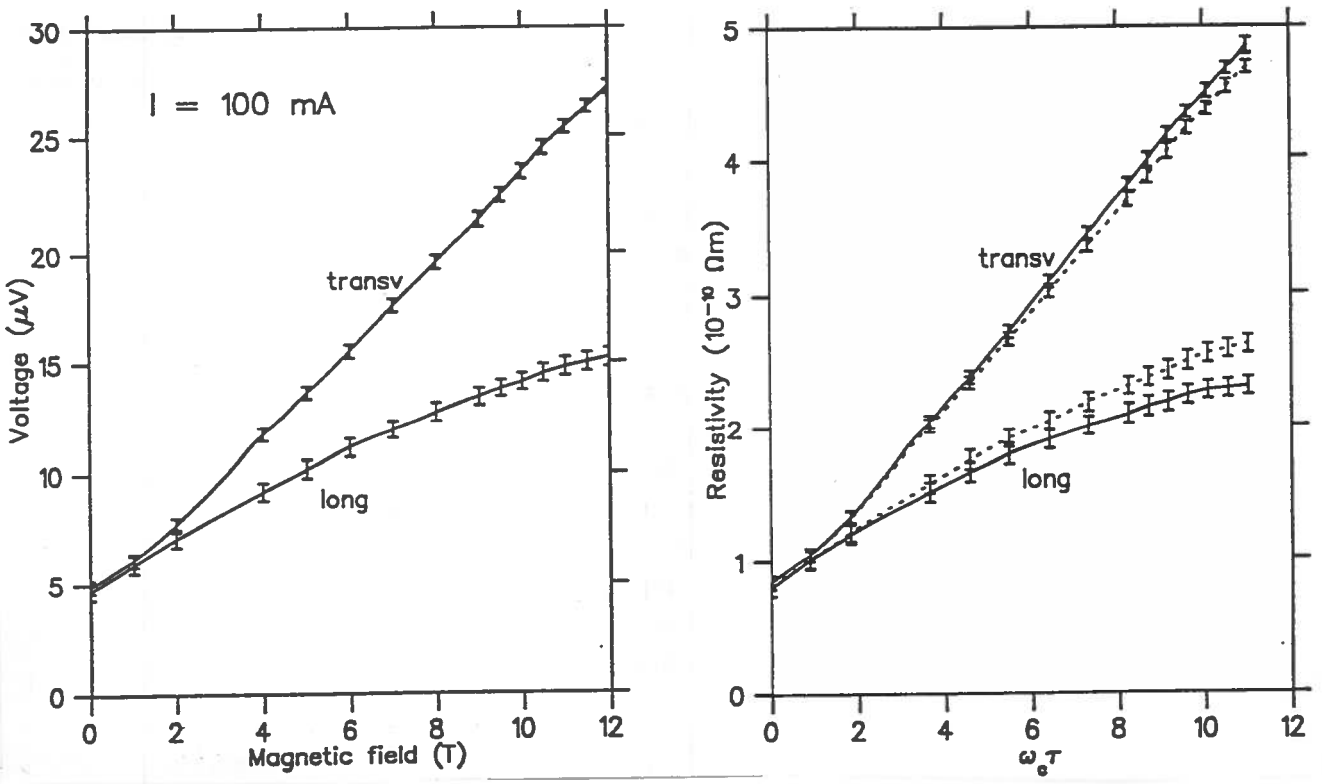

Figure 7: *First copper wire (0.5 mm dia. RRR=182) at $T = 4.17 \pm 0.05\ K$. On the left, measured voltage, on the right, resistivity. This has been calculated using only one kind of measurements each time (dotted line), and using both kinds and the system shown before, in order to separate the two components (solid line).*

All measurements have been done measuring the offset (V_0) when no current was flowing in the sample. The offset was about 4 μV and its variation during each measurement (δV_0) no more than 0.3 μV. For each field value measurements have been repeated 5 times. Voltages plotted in figure 7 refer to a 100 mA current. In the same figure also the resistivity is shown, calculated both with (full lines) and without (dotted lines) using the system to separate components. The values of $\omega_c\tau$ have been calculated using this relation: $\omega_c\tau = B\sigma_0/ne$ where n is the electron density, e the electron charge and σ_0 is at 4.2 K. It can be seen that transverse magnetoresistance increase is linear while there is a tendency to saturation for the longitudinal magnetoresistance. Both behaviours agree with theoretical predictions and with measurements present in literature.

Transversal resistivity values are $\rho_{12T} = 4.86\ 10^{-10}$ Ωm at 12 tesla and $\rho_0 = 0.846\ 10^{-10}$ Ωm at 0 tesla, so it is $\frac{\Delta\rho}{\rho_0} = 4.7$.

The residual resistance ratio (RRR) is 182 and so B*RRR is 2184. Those two values agree quite well with Kohler curve for transverse magnetoresistance in polycrystalline copper.

The second sample has a diameter of 0.127 mm and a length of 118 mm. Its resistance at room temperature is 156 mΩ and so its resistivity is $1.67\ 10^{-8}$ Ωm. Measurements have been done at these temperatures: $9.12 \pm 0.04\ K$, $4.15 \pm 0.05\ K$ and $1.97 \pm 0.05\ K$. Different currents have been used: 25, 50, 75 mA, but no differences have been seen.

Voltage spanned from 84 to 360 μV using a 50 mA current; the offset V_0 was very high, about 20 μV and was not constant showing a great field dependence with oscillation (δV_0) up to 12 μV. Measurements have been repeated 5 times for each field value and the spread among measures showed again an increase with the field. These voltage oscillations are

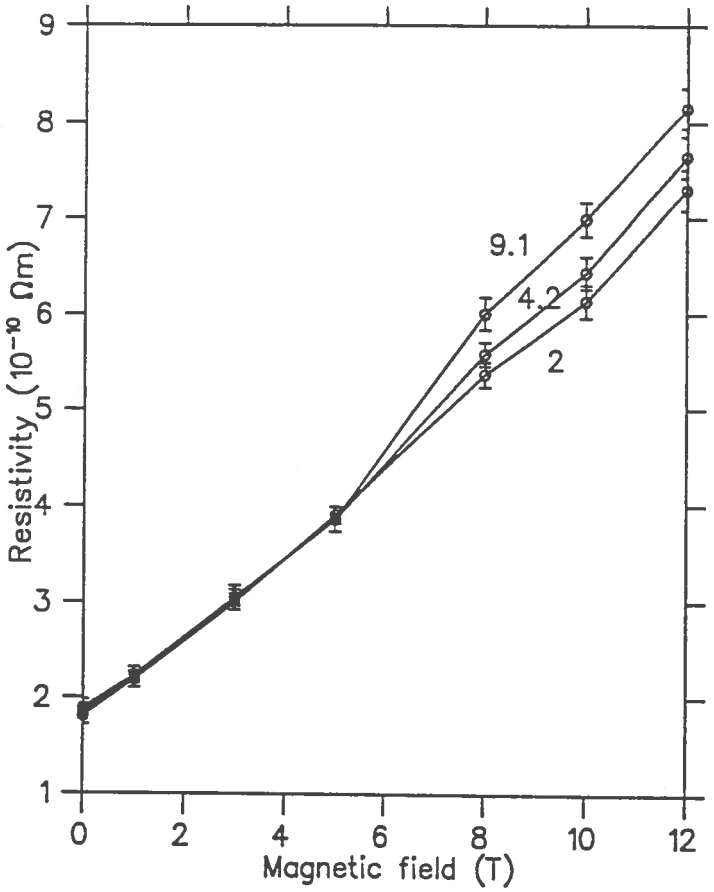

Figure 8: *Transversal magnetoresistance of the second copper sample at different temperatures.*

Table 3: *Second copper sample (0.127 mm dia.) data for transversal magnetoresistance Kohler plot.*

Temperature (K)	RRR(t)	$\Delta\rho/\rho$	B×RRR(t)
1.94	92.8	3.05	1114
4.17	90.7	3.14	1089
9.04	88.6	3.32	1064

supposed to be an effect of sample oscillations.

Transversal magnetoresistance is shown in fig. 8 and it can be seen that the three curves separate for fields greater than 5 tesla. This behaviour can be explained as a small-angle scattering effect[11]. In table 3 the residual resistance ratios and the $\frac{\Delta\rho}{\rho_0}$ values are shown. They all agree with Kohler curve for polycrystalline copper. For this sample the value of $\omega_c\tau$ at 12 tesla is 4.9.

4.2 NbTi samples

NbTi samples used have been two wires with diameters of 33 μm and 13 μm. Measurements have been done at different temperatures, from 4.2 to 11 K in order to see both transitions curves and magnetoresistance behaviour. All measurements have been done with sample holder in longitudinal and transversal position, and no differences depending on sample

[11]See pag. 5.

Table 4: *Temperature variations during measurements on first NbTi wire.*

Current (mA)	Temperature (K)	Variation (K)
1.486	11.12	±0.05
1.486	9.05	±0.02
1.486	6.97	±0.02
1.486	6.02	±0.03
1.486	4.24	±0.02
0.4998	9.05	±0.02
0.4998	7.98	±0.02
0.4998	7.01	±0.01
0.4998	6.02	±0.02
0.4998	5.00	±0.04

orientation have been detected.

First sample used is a NbTi wire (33 μm diameter and 107 mm length) with 46 % Ti made by Vacuumschmelze (Hanau - D). Its resistance and resistivity are 56 Ω and 4.48 10^{-7} Ωm at room temperature, and 48 Ω and 3.84 10^{-7} Ωm at 77 K.

Measurements have been done at 11, 9, 8, 7, 6, 5, and 4.2 K using first a current of 1.486 mA and then a current of 0.4996 mA. Comparing normal state resistivity measured with different currents no differences can be detected, while a small difference appears (when overlapped) in the transition curves: it's probably a tiny self-heating effect even if can also be explained with a variation of the bath temperature of 10≈20 mK).

All measurements are shown in figure 9. Measurements have been repeated 5 times for each field value in order to calculate the mean value and the error. Temperatures and their variations are shown in table 4.

In figure 10 only magnetoresistance at 11 K is shown with the sample holder in both longitudinal and transverse position. Together with the measured points the best fits using a cubic polynomial $y = a_0 + a_1 x + a_2 x^2 + a_3 x^3$ are plotted. It can be seen that both longitudinal and transverse magnetoresistance tend to saturate, and that their behaviour is almost equal. $\frac{\Delta\rho}{\rho_0}$ is 2.13 10^{-3}, a very little value, but this is not surprising since also the RRR value is very small: 1.37. This is due to the great number of impurities present in a superconducting filament with strong pinning characteristics.

During these measurements V_0 oscillated between 3.5 and 5.5 μV, while the difference between voltages measured at 12 tesla and at 0 tesla is 134 μV ($V_{12\,T}$ = 61.050 mV, $V_{0\,T}$ = 60.916 mV), that is 67 times greater than δV_0.

The second superconducting sample we used is a NbTi filament with diameter of 13 μm and length of 107 mm, of the same type of filaments used for the superconducting dipoles of Hera (the accelerator in Amburg at Desy laboratory), made by EM - LMI (Florence).

Its resistance at room temperature is 313 Ω and so its resistivity is 3.88 10^{-7} Ωm. Measurements have been done at different temperatures from 5 to 11 K (see table 5), using a current of I = 0.1248 mA. In figure 11 all measurements are shown. Error bars don't appear because they are smaller than the plotting symbol. This is due to the use of a better power supply.

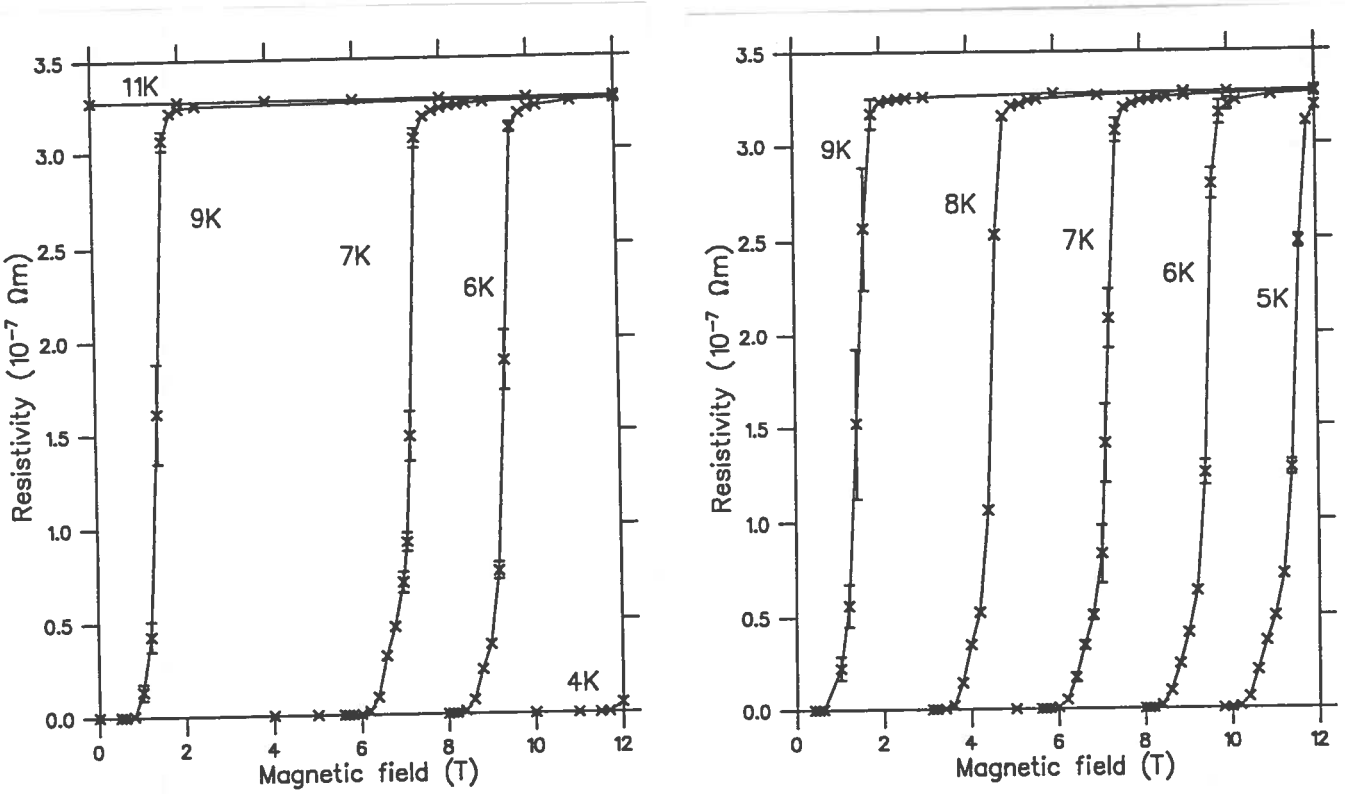

Figure 9: *All measurements on first NbTi wire (Ø=33 μm). On the left I=1.486 mA, on the right I=0.4998 mA. See text for comments.*

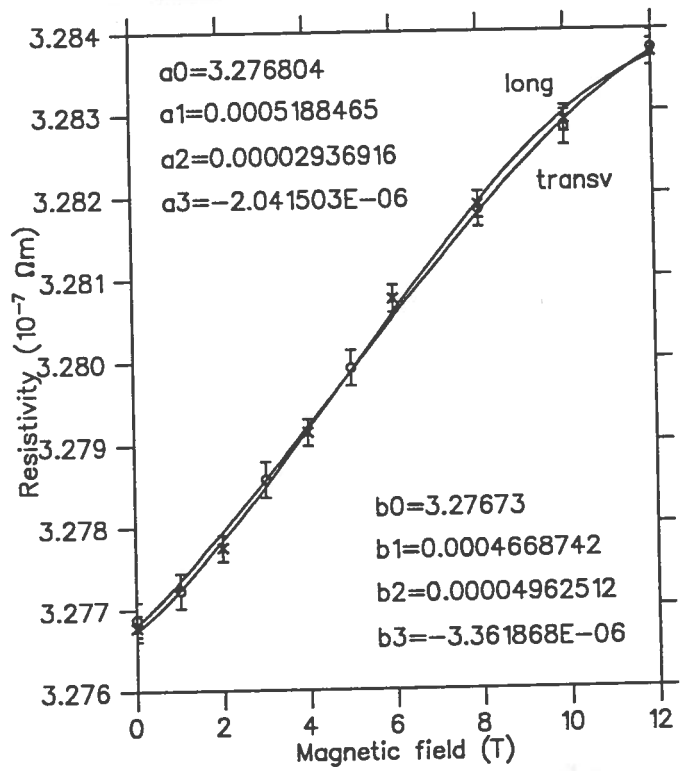

Figure 10: *Magnetoresistance of first NbTi wire (Ø=33 μm), at 11.1 K with parameters of the fit* $y = a_0+a_1x+a_2x^2+a_3x^3$ *for transverse magnetoresistance and* $y = b_0+b_1x+b_2x^2+b_3x^3$ *for longitudinal magnetoresistance .*

Table 5: *Temperature variations during measurements on second NbTi wire.*

Temperature (K)	Variation (K)
11.02	±0.01
9.07	±0.01
8.06	±0.02
7.00	±0.01
5.90	±0.02
4.84	±0.01

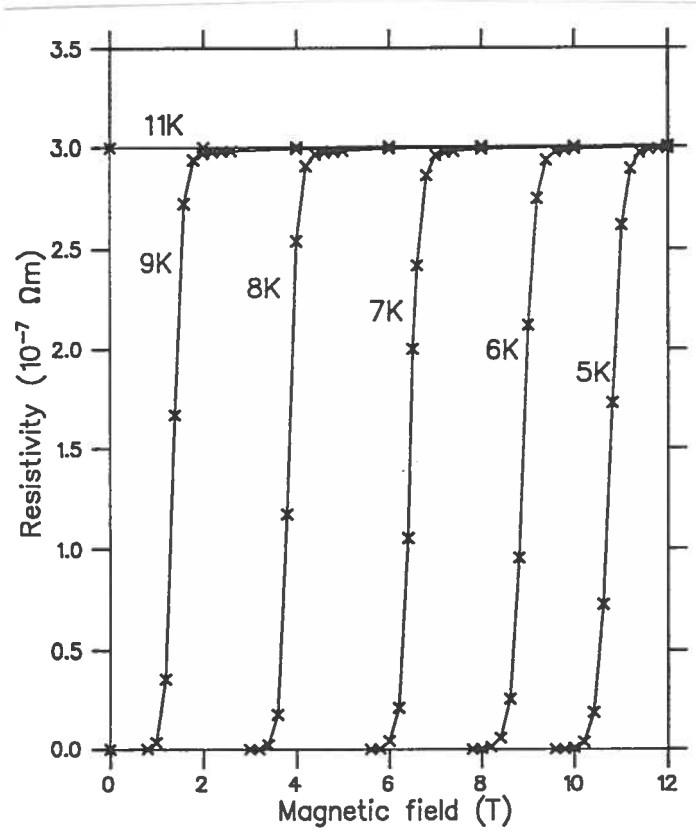

Figure 11: *All measurements on second NbTi wire (Ø=13 μm).*

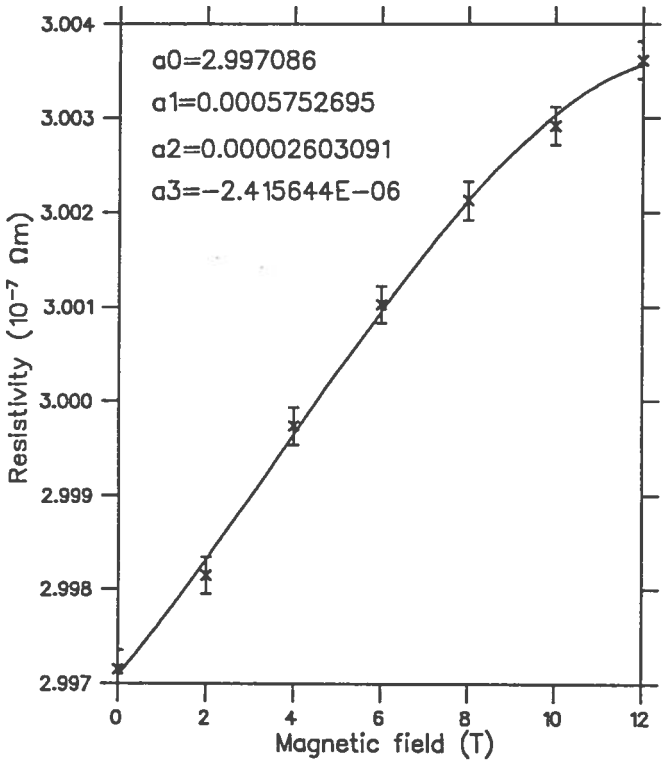

Figure 12: *Transverse magnetoresistance of second NbTi wire (Ø=13 μm), at 11 K and parameters for the fit* $y = a_0 + a_1x + a_2x^2 + a_3x^3$.

In figure 12 transverse magnetoresistance at 11 K is shown with values for the best fitting using a cubic polynomial : $y = a_0 + a_1x + a_2x^2 + a_3x^3$. For this sample $\frac{\Delta\rho}{\rho_0}$ is 2.16 10^{-3} while the RRR value is 1.30. The difference between voltage measured at 12 tesla and at 0 tesla is 65 μV ($V_{12\,T} = 30.218$ mV, $V_{0\,T} = 30.153$ mV), while V_0 oscillated during measurements from 4.5 to 4.7 μV. The noise, δV_0, is then about 0.3 % of the signal ΔV due to magnetoresistance.

5 Conclusions

The measurements on copper wires and on NbTi filaments show that the apparatus enables us to measure the magnetoresistance in a wide range of temperature and magnetic field, with an accuracy of few percents. As shown by measurements on the last NbTi sample, the accuracy can be easily increased to 0.1 % by using a proper power supply without ripple.

While the apparatus is being used for technical material (like copper and aluminium used as stabilising material in superconducting cables), a minor modification, in order to accommodate filaments thinner than 10 μm like the ones needed for the LHC dipoles, is in progress.

As for the results obtained with the 33 μm and 17 μm NbTi filaments we can say that no size effect has been detected, so nothing can be said about sausaging by means of magnetoresistance measurements. We believe that this technique may give useful informations if the filaments are in the micron and submicron range.

Figure 13: *A part of the instrumentation: a multimeter used to monitor temperature inside the magnet (using two Rh-Fe sensors), the nanovoltmeter, liquid helium and liquid nitrogen level controllers, the temperature controller for the V.T.I..*

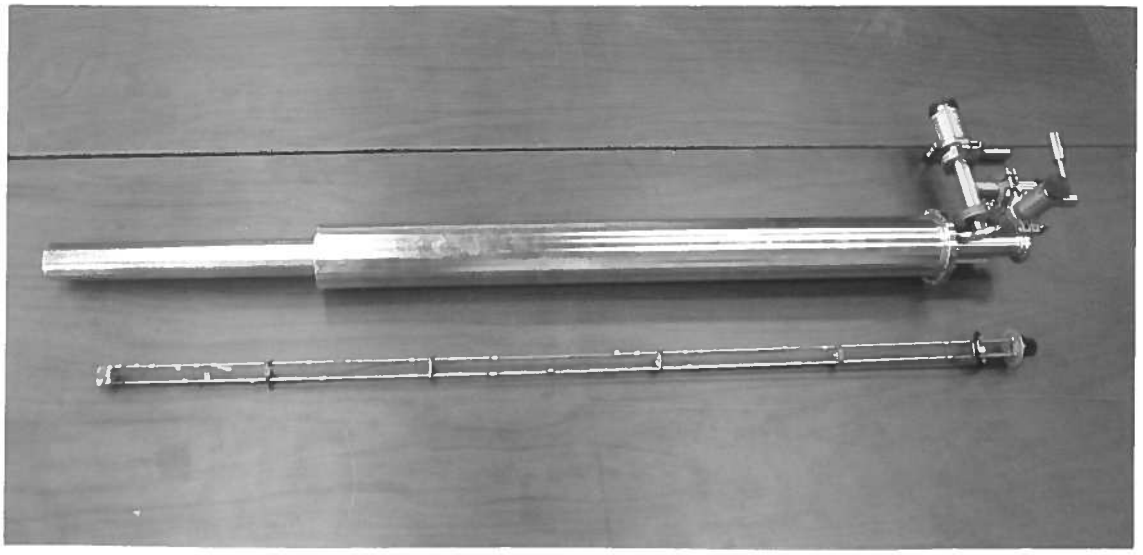

Figure 14: *The variable temperature insert and the support for the sample-holder.*

Figure 15: *The superconducting magnet with the V.T.I. inside it. On the top flange of the cryostat four service lines can be seen. From left to right turning clock-wise: the evacuation line for the VTI vacuum chamber, the helium gas exhaust line for the magnet, the pumping line for the sample chamber, and the line coming from the λ-point refrigerator.*

Acknowledgements

The authors gratefully acknowledge the contribution of Dr. Li Baozeng visitor from Inst. of Plasma Physics, Hefei, China, and Mr. A. Leone for his valuable assistance in vacuum systems and cryogenics.

References

[1] E. Acerbi et al. *"State of the construction of two INFN full length superconducting dipole prototype magnets for the Large Hadron Collider (LHC)", Proc. of III EPAC*, Berlin, March 1992, Edition Frontier 1992, p.1420.

[2] E. Acerbi et al. *"Italian development of a superconducting cable for the main dipoles of the Large Hadron Collider", Proc. of III EPAC*, Berlin, March 1992, Edition Frontier 1992, p.1417.

[3] I.M. Lifshitz, M.Ya. Azbel' and M.I. Kaganov, *J.E.T.P.* 3, 143 (1956) and 4, 41 (1957).

[4] A.B. Pippard, *"Magnetoresistance in metals"*, Cambridge University Press, 1989.

[5] J.M. Ziman, *Phil. Mag.* 3, 1117 (1958).

[6] A.B. Pippard, *Phil. Trans. Roy. Soc.* A291, 569 (1979).

[7] J. de Launay, R.L. Dolecek and R.T. Webber, *J. Phys. Chem. Solids* 11, 37 (1959).